# Photonic properties of Er-doped crystalline silicon

Vinh, N.Q.; Ha, N.N.; Gregorkiewicz, T.

DOI
10.1109/JPROC.2009.2018220
Publication date
2009
Document Version
Final published version
Published in
Proceedings of the IEEE

INVITED PAPER

# Photonic Properties of Er-Doped Crystalline Silicon

*Multilayer nanostructure devices, built with silicon crystals doped with rare-earth ions, open new possibilities for light-emitting devices in on-chip optical interconnects.*

By Nguyen Quang Vinh, Ngo Ngoc Ha, and Tom Gregorkiewicz

**ABSTRACT** | During the last four decades, a remarkable research effort has been made to understand the physical properties of Si:Er material, as it is considered to be a promising approach towards improving the optical properties of crystalline Si. In this paper, we present a summary of the most important results of that research. In the second part, we give a more detailed description of the properties of Si/Si:Er multinanolayer structures, which in many aspects represent the most advanced form of Er-doped crystalline Si with prospects for applications in Si photonics.

**KEYWORDS** | Erbium; excitation; luminescence; nanolayers; optical gain; photonic; radiative recombination; rare earth; silicon; terahertz; two-color spectroscopy

## I. Er-DOPED BULK CRYSTALLINE SILICON

### A. Introduction

*1) Rare Earth Ions as Optical Dopants:* Doping with rare-earth (RE) ions offers the possibility of creating an optical system whose emissions are characterized by sharp, atomic-like spectra with predictable and temperature-independent wavelengths. For that reason, RE-doped matrices are frequently used as laser materials (large bandgap hosts, e.g., Nd:YAG) and for optoelectronic applications (semiconducting hosts) [1]–[3]. Very attractive features of RE ions follow from the fact that their emissions are due to internal transitions in the partially filled 4*f*-electron shell. This core shell is effectively screened by the more extended 5*s*- and 5*p*-orbitals. Consequently, the optical and also magnetic properties of an RE ion are relatively independent of a particular host. All RE elements have a similar atomic configuration $[Xe]4f^{n+1}6s^2$ with n = 1–13. Upon incorporation into a solid, RE dopants generally tend to modify their electronic structure in such a way that the 4*f*-electron shell takes the $[Xe]4f^n$ electronic configuration, characteristic of trivalent RE ions. We note that this electronic transformation does not imply triple ionization of an RE ion, and can arise due to bonding—as is the case for Yb-doped InP, where the $Yb^{3+}$ ion substitutes for $In^{3+}$, or due to a general effect of the crystal environment—as for Er in Si discussed here.

*2) RE Doping of Semiconductors:* In addition to the predictable optical properties and, in particular, the fixed wavelength of emission, RE-doped semiconductor hosts offer yet one more important advantage, that is, RE dopants can be excited not only by a direct absorption of energy into the 4*f*-electron core but also indirectly, by energy transfer from the host. This can be triggered by optical band-to-band excitation, giving rise to photoluminescence (PL); or by electrical carrier injection—electroluminescence (EL). Among many possible RE-doped semiconductor systems, research interest has been mostly concentrated on Yb in InP and Er in Si. $Yb^{3+}$ is attractive for fundamental research due to its simplicity—its electronic configuration of $4f^{13}$ features only a single hole, thus giving rise to a single excited state [4]. Moreover, emission from $Yb^{3+}$ in InP is practically independent from sample preparation procedures, since $Yb^{3+}$ always tends to take the well-defined lattice position substituting for $In^{3+}$.

Manuscript received February 5, 2009. Current version published June 12, 2009.
**N. Q. Vinh** is with the Van der Waals-Zeeman Institute, University of Amsterdam, NL-1018 XE Amsterdam, The Netherlands. He is also with the FOM Institute for Plasma Physics Rijnhuizen, NL-3430 BE Nieuwegein, The Netherlands (e-mail: vinh@itst.ucsb.edu).
**N. N. Ha** and **T. Gregorkiewicz** are with the Van der Waals-Zeeman Institute, University of Amsterdam, NL-1018 XE Amsterdam, The Netherlands (e-mail: N.H.Ngo@uva.nl; t.gregorkiewicz@uva.nl).
Digital Object Identifier: 10.1109/JPROC.2009.2018220

For Si:Er [5], [6], the interest has been fueled by prospective applications for Si-photonics, in view of the full compatibility of Er doping with CMOS technology. Upon its identification, Er-doped crystalline Si (c-Si:Er) emerged as a perfect system where the most advanced and successful Si technology could be used to manufacture optical elements whose emission coincides with the 1.5 $\mu$m minimum absorption band of silica fibers currently used in telecommunications. Unfortunately, in sharp contrast to that bright prospect, c-Si:Er proved to be notoriously difficult to understand and to engineer. Consequently, while a lot of progress has been made, four decades after the first demonstration of PL from Si:Er, efficient room-temperature light-emitting devices based on this material are still not readily available.

### B. $Er^{3+}$ Ion as a Dopant in Crystalline Si

*1) Incorporation:* One of the major problems in the way of efficient emission from c-Si:Er—both under optical and electrical excitation—is the low solubility of Er in c-Si and the multiplicity of centers that Er forms in the Si host. This follows directly from the fact that Er is not a "good" dopant for c-Si, as it tends to take 3+ rather than the 4+ valence characteristic of the Si lattice, and its ionic radius is very different from that of Si. Moreover, due to the closed character of external electron shells, the 4*f*-orbitals do not bind with the $sp^3$ hybrids of Si. Therefore, in a striking contrast to the aforementioned case of Yb in InP, Er dopants do not occupy well-defined substitutional sites. This leads to a certain randomness of Er positioning in the Si host, with a large number of possible local environments and a variety of local crystal fields. Consequently, while photons emitted from "individual" $Er^{3+}$ ions are very well defined, the ensemble spectrum from a c-Si:Er sample is inhomogeneously broadened. This leads to the situation where a photon emitted by one Er center is not in resonance with transitions of another one and, as such, cannot be absorbed. Combined with the small absorption cross-section of $Er^{3+}$, this makes realization of optical gain in c-Si:Er very challenging.

In view of the long radiative lifetime (milliseconds) of the first $^4I_{13/2}$ excited state of $Er^{3+}$, a large concentration of Er is desirable in order to maximize the emission intensity. This is, however, precluded by the low solid-state solubility of Er in c-Si. Therefore, nonequilibrium methods are commonly used for preparation of Er-doped Si. The best results have been obtained with ion implantation [7] and molecular beam epitaxy (MBE) [8] or sublimation MBE (SMBE) [9], [10]. Sputtering and diffusion are also occasionally used for preparation of Er-doped structures [11]. With nonequilibrium doping techniques, Er concentrations as high as $[Er] \approx 10^{19}$ cm$^{-3}$ have been realized. Such high doping concentrations bring a problem of reduction in "optical activity" of Er dopants. It has been observed that only a small part of the high Er concentration—typically ~1%—contributes to photon emission. Possible reasons for this unwelcome effect include the segregation of Er to the surface, clustering into metallic inclusions, and "concentration quenching." In addition to these, it has been postulated that in order to attain optical activity, i.e., the ability to emit 1.5 $\mu$m radiation, the $Er^{3+}$ ion must form an "optical center" of a particular microscopic structure. Since codoping with electronegative elements, in particular with oxygen, can substantially increase the optical activity of Er in Si, it was postulated that such an optical center should contain oxygen atoms.

*2) Microscopic Aspects:* The energetic structure of an $Er^{3+}$ ion incorporated in c-Si can be determined following the Russell–Saunders scheme, with the spin-orbit interaction resulting in $^4I_{15/2}$ and $^4I_{13/2}$ as the ground and the first excited states respectively, and higher lying $^4I_{11/2}$ and $^4I_{9/2}$ states. Transitions between the ground and the first excited states can be realized within the energy determined by the Si bandgap.

The actual symmetry of the optically active Er center in c-Si remains somewhat controversial and clearly varies according to the presence and the chemical nature of codopants. Early PL studies of the 1.5 $\mu$m emission in Si [12] drew a confusing picture of $Er^{3+}$ ions in the sites of tetrahedral symmetry $T_d$ (substitutional or interstitial). A subsequent investigation with a high-resolution PL study has identified more than 100 emission lines [2]. These were assigned to several simultaneously present Er-related centers with different crystal surroundings, including isolated $Er^{3+}$ ions at interstitial sites, Er-O complexes, Er complexes with residual radiation defects, and isolated $Er^{3+}$ ions at sites of different symmetries.

Extended X-ray absorption fine structure spectroscopy [13] revealed the presence of six oxygen atoms in the immediate surrounding of the local site of an Er atom in Czochralski (Cz) Cz-Si:Er [13], [14] and 12 Si atoms in float-zoned (Fz) Fz-Si:Er. These findings were confirmed by Rutherford back-scattering [15] and electron paramagnetic resonance studies [16]. Channeling experiments by Wahl *et al.* [17] identified the formation of an Er-related cubic center at a tetrahedral interstitial site ($T_i$) as the main center generated in c-Si by Er implantation. This finding was in agreement with the first theoretical calculations predicting a tetrahedral interstitial location of an isolated $Er^{3+}$ ion in Si [14], [18]–[23]. Although some found a tetrahedral substitutional site ($T_S$) of $Er^{3+}$ ions to be more stable [21], [23], others calculated that the hexagonal interstitial site ($H_i$) has the lowest energy [14], [19].

*3) Role of Oxygen:* It is known empirically that the solubility of Er in c-Si and its PL intensity can be efficiently enhanced by codoping with oxygen. This effect is optimal for an oxygen-to-erbium doping ratio of approximately 10 : 1 and an Er concentration of $10^{19}$ cm$^{-3}$ [24], [25]. O atoms play at least two roles in the c-Si:Er system. First, O can

greatly lower the binding energy due to the interactions between O and Si, and also O and Er, atoms, thus enabling the incorporation of Er into Si. Secondly, the presence of O modifies the c-Si:Er electrical properties [26], [27]. In fact, it has been shown that while Er in c-Si exhibits donor behavior, the maximum donor concentration obtained for a fixed Er content is much higher in Cz-Si than in Fz-Si.

*4) Electrical Activity:* The formation of electrical levels within the host bandgap has a crucial importance for optical activity of RE dopants. In general, the trivalent character indicates that in III–V compounds, RE ions may form isoelectronic traps. In the InP:Yb system, it is accepted that the substitutional $Yb^{3+}$ ion generates a shallow donor level with an ionization energy of approximately 30–40 meV [4], [28], [29], although the detailed origin of the binding potential has not been clearly established [18]. In that case, the RE ion is neutral with respect to the lattice and the negatively charged trap attracts a hole; hence, an "isoelectronically" bound exciton state is formed [30], [31]. With that state, energy transfer to the 4*f*-shell is possible in a process similar to the nonradiative quenching of excitons bound to neutral donors (three particle process). The excess energy is emitted as phonons. It is quite likely that a similar situation takes place also for c-Si:Er [32]. Here this process is more complex, as, in principle, the substitutional $Er^{3+}$ should give rise to an acceptor level. The 3+ charge state of the core suggests the formation of an acceptor state in Si when on a substitutional site. More generally, the existence of a coulombic potential opens a possibility for the formation of effective-mass hydrogenic donor or acceptor states. However, these were not detected in experiments.

It is commonly observed that the Si crystal usually converts to *n*-type upon Er doping. Accordingly, a donor level at approximately 150 meV below the conduction band has been detected by deep level transient spectroscopy (DLTS) in oxygen-rich Cz-Si:Er [33]. As a possible reason for this, the mixing of the *d* states of $Er^{3+}$ ion with conduction band states of Si [18] and the formation of erbium-oxygen [33] or erbium-silicide clusters [34] were proposed. However, the electrical measurements are not able to discriminate between optically active and nonactive fractions of Er dopants. Therefore, the link between formation of a donor level and the ability to emit a photon by $Er^{3+}$ is indirect. As will be discussed in Section II-B5, a direct relation between the formation of a particular donor center and optical activity has only recently been established by a combination of two-color and PL excitation (PLE) spectroscopies for a particular Er-center created in a Si/Si:Er multinanolayer structure [35].

### C. Excitation Process of Er in Crystalline Si

*1) Introduction:* The external screening of the 4*f*-electron shell, which determines attractive features of the Er-related emission, presents a considerable disadvantage for the excitation process. In RE-doped ionic hosts and molecular systems, the excitation transfer usually proceeds by energy exchange between an RE ion, acting as an energy acceptor, and a radiative recombination center—an energy donor. In that case, the first step is the excitation of the energy donor center. Subsequently, the energy is nonradiatively transferred via the multipolar or exchange mechanism to the 4*f*-shell of an RE ion, with an eventual energy mismatch being compensated by phonons. In a semiconducting host, the first excitation stage involves host band states (exciton generation) and is usually very efficient. The subsequent energy transfer to (and similarly from) a RE ion depends crucially on the availability of traps allowing the creation of a bound exciton state in the direct vicinity of the RE ion (Fig. 1). Therefore, the excitation process changes dramatically if the RE ion itself introduces a level within the band gap of the host material. The electrical activity of Er in Si and, in particular, the formation and the characteristics of an Er-related donor level essential for the properties of Si:Er were discussed in Section I-B4. An electron captured at the donor level can subsequently recombine nonradiatively with a free hole from the valence band, or with a hole localized in the effective-mass potential induced by the trapped electron, and transfer energy to the 4*f*-shell of an $Er^{3+}$ ion. The energy mismatch can be accommodated by phonon emission. In a somewhat different model [36], the initial localization of an electron at the Er-related donor level creates an effective exciton trap. In this case, an electron-electron-hole system is created upon binding of an exciton and the excess energy during the core excitation process can now be absorbed by the second electron, which is released from the donor level into the conduction band.

*2) Multi-Stage Excitation Process:* In general, the Er-related luminescence in Si can be induced electrically, by carrier injection, or optically with the photon energy exceeding the energy gap. The excitation proceeds indirectly via one of two different Auger-type energy transfer

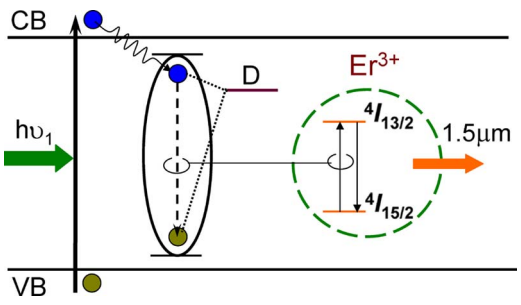


**Fig. 1.** *Model for photo-excitation of $Er^{3+}$ doped crystalline Si system, where CB, VB, and D stand for conduction band, valence band, and donor level, respectively.*

processes. In EL, Er excitation is accomplished either by collision with hot electrons from the conduction band under reverse bias, or by generation of electron-hole pairs in a forward biased $p-n$ junction. The electronic collision under reverse bias has been recognized as the most efficient excitation procedure for c-Si:Er. In PL, energy transfer to the 4*f*-electron core is accomplished by nonradiative recombination of an exciton bound in the proximity of an $Er^{3+}$ ion, as discussed in the previous section. This multi-stage optical excitation mechanism for c-Si:Er has been investigated experimentally and by theoretical modeling [32], [36]–[39]. In particular, the importance of excitons [40] and the enabling role of the Er-related donor [35] have been explicitly demonstrated. With the proposed models, the Er-related PL intensity dependence on both temperature and excitation power were successfully described [41]. The effective cross section for the indirect excitation mode is of the order of $\sigma \approx 10^{-14}$ cm$^2$, i.e., much higher (factor $\sim 10^6$) than under direct resonant photon absorption by $Er^{3+}$ ions[1] [42]. This large difference evidences the advantage of the semiconducting Si matrix for the excitation process. Perhaps the most straight forward evidence for the multi-stage excitation process of $Er^{3+}$ ions came from two-color experiments [43], [44] in which the electron and hole necessary for that process were supplied in two separate processes. In this case, capture of one type of carrier at an Er-related state formes a stable stage in which $Er^{3+}$ ion is "prepared" for excitation upon subsequent availability of the complementary carrier.

Interesting insights into the excitation process have been obtained by investigating the emission from an Er-implanted sample measured in different configurations of optical excitation [40]. Comparison of PL recorded with a laser beam incident on the implanted-side and on the substrate-side of the sample gives evidence that energy is being transported to $Er^{3+}$ ions by excitons, and that the efficiency of this step strongly depends on the distance between the photon absorption region, where excitons are generated, and $Er^{3+}$ ions, as indeed intuitively anticipated [42].

*3) Alternative Recombination Paths Influencing Er Excitation Process:* In view of the complex character of the excitation process, the centers whose presence in the material is not directly related to $Er^{3+}$ ions, e.g., shallow level doping, implantation, and growth/deposition damage, etc., exert a profound influence on the energy flow. In particular, alternative relaxation paths may appear at every stage of the process, strongly affecting its final efficiency. These effects can be visualized when comparing the excitation process in undoped Si and upon the presence of shallow states providing competing exciton traps. For Er-doped Si:P, it has been demonstrated [45] that application of an electric field can block energy relaxation through shallow donor phosphorus, thus channeling it to Er and enhancing its excitation efficiency. This result shows that phosphorus donors and Er-related centers compete in exciton localization. In addition, it also provides direct evidence that the exciton binding energy is bigger for Er-related traps than for P, suggesting larger ionization energy of the relevant donor center.

An alternative recombination is also possible at the aforementioned bound exciton state mediating the host-to-Er energy flow. Such a process involves energy transfer to free carriers (Auger type) and is identical to that facilitating the major channel of nonradiative recombination for excited $Er^{3+}$ ions (next section). More generally, an Auger process involving energy transfer to free carriers is known to be the most efficient quenching mechanism in the luminescence of localized centers [46]. The free-carrier mediated mechanism lowering the Er excitation efficiency was confirmed in a two-color experiment allowing to adjust the equilibrium concentration of free carriers [47].

*4) Other Possible Excitation Mechanisms:* In addition to the above outlined more "standard" energy transfer mechanisms resulting in promotion of an $Er^{3+}$ ion into its first $^4I_{13/2}$ excited state, direct formation of the next higher lying $^4I_{11/2}$ state has also been considered. It appears indeed plausible to reach this state via the second conduction sub-band of c-Si [32] and such a process could be quite efficient due to the energy match and, consequently, its very nearly resonant character. In particular, it has been speculated that pumping into the second excited state might be realized under intense carrier heating with an infrared (IR) laser [48], and experimental support for that has been found in investigations of c-Si:Er in strong laser fields. A very similar mechanism has been also used to explain the temperature dependence of emission intensity for c-Si:Er based light-emitting diode structures [49]. In this case, the activation of this new mechanism was accomplished thermally. We note that excitation into the $^4I_{11/2}$ state is commonly realized in a similar and well-investigated system-$SiO_2$:Er sensitized with Si nanocrystals [50]–[52].

### D. De-Excitation Processes of Er in Crystalline Si

*1) Introduction: Radiative Recombination:* The radiative transition probability between the 4*f*-shell derived energy states is usually very small. Theoretically, for an RE ion in vacuum, transitions between different multiplets originating from the 4*f*-electron shell are forbidden for parity reasons. Upon incorporation in a matrix, the local crystal field leads to a small perturbation of these states and nonzero transition matrix elements appear. However, as discussed before, this effect is small due to screening; therefore the transitions are only slightly allowed and recombination times $\tau$ remain long—in the millisecond range. In an extreme case, for $Er^{3+}$ in an insulating host

[1]We note that the $\sigma_{eff} \approx 4 \times 10^{-12}$ cm$^2$ given in [37] follows from a numerical error, and should be $\sigma_{eff} \approx 4 \times 10^{-14}$ cm$^2$; see [42].

$Cs_2NaYF_6$, $\tau \approx 100$ ms has been measured for the first excited state $^4I_{13/2}$ [53]. The radiative lifetime for Er in $SiO_2$ has been estimated as $\tau \approx 22$ ms [54]. For Er in c-Si, the longest reported lifetime of $\tau \approx 2$ ms has been experimentally determined for *p*-type Cz-Si at $T = 15$ K [37].

*2) Thermal Quenching:* Upon temperature increase, nonradiative recombinations appear and dominate the Er de-excitation processes. This is experimentally observed as thermally-induced quenching of both the PL intensity and the effective lifetime [41]. We recall that in the EL of some Si:Er-based structures the so-called "abnormal" thermal quenching has been reported [55]. This was related to changes in the impact excitation mode, with the temperature-induced transition from avalanche to the more efficient electron tunneling current. In such a case, the efficiency of Er excitation increases with temperature, masking the gradual rise of thermally activated nonradiative recombination channels.

For RE ions in insulating hosts, the nonradiative recombination is usually dominated either by multiphonon relaxation or by a variety of energy transfer phenomena to other RE ions. The presence of delocalized carriers (either free or weakly bound) in semiconductors opens new channels specific for these materials. Below, we discuss the two most important of them: the so-called "back-transfer" process in which the excitation process is reversed, and energy dissipation to free carriers, which are promoted to higher band-states.

*3) Back-Transfer Process of Excitation Reversal:* The back-transfer process originally proposed for InP:Yb [56] is generally held responsible for the high-temperature quenching of the RE PL intensity and lifetime. The low probability of radiative recombination makes the back-transfer process possible with the necessary energy being provided by simultaneous absorption of several lattice phonons. During the back-transfer, the last step of the excitation process is reversed: upon nonradiative relaxation of an RE ion, the intermediate excitation stage (the bound-exciton state) is recreated. The activation energy of such a process is equal to the energy mismatch that has to be overcome and therefore depends on the gap position of the aforementioned RE-related donor state. For InP:Yb, the back-transfer process was demonstrated to be induced also optically, under intense illumination of IR photons with the appropriate quantum energy [57]. For c-Si:Er, the energy necessary to activate the back-transfer process is $\Delta E \approx 150$ meV and therefore the participation of at least three optical phonons is required. Investigations of thermal quenching of the PL intensity and lifetime in c-Si:Er reported two activation energies: $\Delta E_1 \approx 15$–$20$ meV and $\Delta E_2 \approx 150$ meV [45]. The former is usually related to exciton ionization or dissociation, and the latter is commonly taken as a fingerprint of the back-transfer process. The multiphonon-assisted back-transfer process for c-Si:Er was modeled theoretically [58] in full agreement with the experimental data.

*4) Auger-Type Energy Transfer to Free Carriers:* As for the excitation mechanism, shallow centers available in the host exert a profound influence on nonradiative relaxation of RE ions. A very effective mechanism of such a nonradiative recombination is the impurity Auger process involving energy transfer to conduction electrons [47]. This process can be seen as opposite to the impact excitation mechanism in EL of c-Si:Er. Direct evidence of the importance of energy transfer to conduction-band electrons was given by an investigation of the temperature quenching of PL intensity for samples with different background doping [37]. In that experiment, the activation energy of thermal quenching directly identified the ionization process of the shallow dopants (B for *p*-type and P for *n*-type) as responsible for this effect.

The detrimental role of free carriers on the emission of c-Si:Er can also be inferred from the fact that free carriers govern the effective lifetime of the excited state of the $Er^{3+}$ ion. This was shown in an experiment where a He-Ne laser, operating in a continuous mode in parallel to the chopped Ar laser, was used to provide an equilibrium background concentration of free carriers. As a result, a shortening of the $Er^{3+}$ lifetime has been observed. The magnitude of this effect was proportional to the square root of the background illumination power [47]. Since the exciton recombination dominated the relaxation, such a result indicates that the efficiency of the lifetime quenching is related to the free-carrier concentration. But possibly the most direct evidence for the Auger quenching of Er PL in Si comes from a two-color experiment in the visible/mid-IR where emission from Er was shown to quench upon the optically induced ionization of shallow traps [59].

## II. Er-1 CENTER IN Si/Si:Er MULTINANOLAYER STRUCTURES

In the previous sections, we have discussed that PL from c-Si:Er reaches maximum quantum efficiency at low temperatures when the excitation of $Er^{3+}$ ions occurs through an intermediate state with the participation of an exciton. This excitation mode may be considerably enhanced in Si/Si:Er multinanolayer structures comprised of interchanged layers of Er-doped and undoped c-Si. Such multinanolayer structures were successfully grown by SMBE [60]. It can be speculated that excitons efficiently generated in a spacer layer of undoped Si have a long lifetime and can diffuse towards Er-doped regions, enabling better excitation of $Er^{3+}$ ions. A multinanolayer structure is schematically depicted in the inset of Fig. 2.

The second part of this review will be dedicated to the electronic and optical properties of Si/Si:Er multinanolayer structures, which emerge as the most promising form of c-Si:Er material.

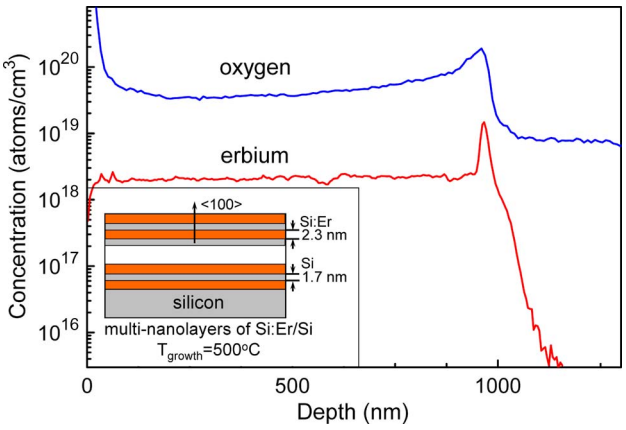


**Fig. 2.** *Secondary ion mass spectroscopy profile for oxygen and erbium concentrations of the investigated SMBE-grown multinanolayer structure, which is schematically illustrated in the inset.*

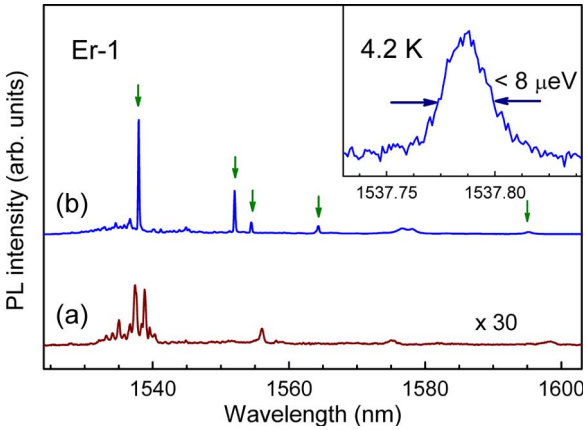


**Fig. 3.** *(a) PL spectra of a Si:Er sample prepared by implantation and (b) SMBE-grown multinanolayers recorded at 4.2 K under $Ar^+$– ion laser excitation. The inset shows the smallest ever measured width of the main peak of SMBE-grown samples.*

### A. Formation of Er-1

*1) Sample Preparation:* The samples whose properties will be discussed consist of 16–400 periods of few-nanometer-thick Si layers alternatively Er-doped and undoped, grown by the SMBE method. For optical activation, annealing of the structures was carried out in a nitrogen or hydrogen flow at 800 °C for 30 min [10], [42], [61]. The concentration of Er in Si:Er layers was $= 3.5 \times 10^{18}$ cm$^{-3}$, as confirmed by secondary ion mass spectroscopy measurements (Fig. 2). While no oxygen was intentionally introduced, a one order of magnitude higher O concentration in the multinanolayer structure than in the Cz-Si substrate has been concluded. For comparison, the properties of an Er and O ion implanted sample (IMPL) (annealed at 900 °C in 30 min in nitrogen) will also be presented [62]. Specifications of the samples whose properties will be discussed are summarized in Table 1.

Er-related emissions are illustrated in Fig. 3. The IMPL sample (trace a) shows numerous lines related to a variety of Er-induced centers. In contrast, the PL spectrum of the SMBE-grown sample (trace b) features only several sharp lines with considerably higher intensities. These are assigned to a specific center called Er-1, marked by arrows [42], [63], [64]. The width of the Er-1 related emission lines (in the inset) is among the smallest ever measured for any emission band in a semiconductor matrix; it is below the experimental resolution of $\Delta E = 8$ $\mu$eV. The measurements also showed that the PL intensity of the Er-1 center increases with the thickness of the spacer layer, up to 50 nm [64].

The Er-1 related PL spectrum has been investigated in detail for temperatures from 4.2 to 160 K. At low temperatures, the Er-1 spectrum consists of a set of five intense lines, labeled $L_1^1$, $L_2^1$, $L_3^1$, $L_4^1$, and $L_5^1$. At higher temperatures, "hot" lines, labeled $L_1^2$, $L_2^2$, and $L_3^2$, appear together with a "second hot" line $L_1^3$—see Fig. 4(a). The intensity ratios of these PL lines are plotted as a function of temperature in Fig. 4(b). Activation energy of $49 \pm 3$ cm$^{-1}$ is determined for all of the intensity ratios of lines $L_x^2$ to $L_x^1$

Table 1 Sample Labels, Parameters, and Annealing Treatments for the Investigated Samples

| Sample label | $d_{Si:Er}$ (nm) | $d_{Si}$ (nm) | $N$ | $\Sigma d_{Si:Er}$ (μm) | $I_{Si:Er}$ (normalized) |
|---|---|---|---|---|---|
| SMBE01 | 2.3 | 1.7 | 400 | 0.92 | 6.6 |
| SMBE02 | 5.0 | 100 | 19 | 0.095 | 49.3 |
| IMPL | 200 | | 1 | | 1 |

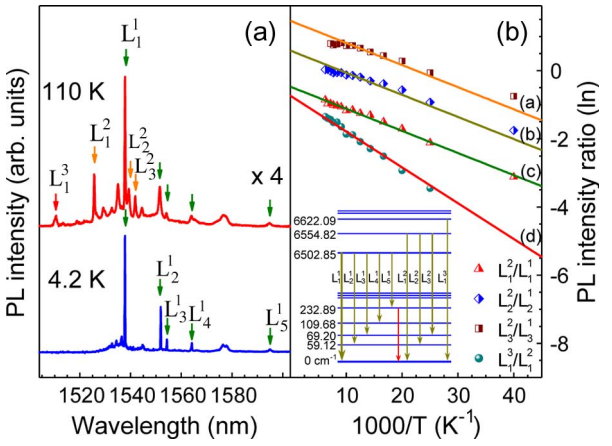


**Fig. 4.** *(a) PL spectra of the multinanolayer structure at 4.2 and 110 K. Arrhenius plots of the temperature variation of the intensity ratios of the hot line $L_1^2$ relative to the line $L_1^1$ (triangles); the hot line $L_2^2$ relative to the line $L_2^1$ (diamonds); the hot line $L_3^2$ relative to the line $L_3^1$ (squares); and the second hot line $L_1^3$ relative to the line $L_1^1$ (circles). The inset illustrates the energy-level splitting of the $J = 15/2$ and $J = 13/2$ manifolds by a crystal field of $C_{2v}$ symmetry.*

("x" is the position of the line in the spectrum). This value is in good agreement with the separation of lines $L_1^2$, $L_2^2$, $L_3^2$ to the lines $L_1^1$, $L_2^1$, $L_3^1$. The intensity ratio of the lines $L_1^3$ to $L_1^2$ has an activation energy of $72 \pm 8$ cm$^{-1}$ (trace d), very similar to their spectroscopic separation. From the temperature dependence of the PL spectrum, we conclude that all its major components thermalize, thus evidencing their common origin from the same center. Consequently, a detailed energy level diagram responsible for the PL of the Er-1 center was developed—see the inset to Fig. 4(b) [64].

*2) Microstructure of Er-1 Center:* Microscopic aspects of the Er-1 center were unraveled in a magnetooptical study [64]–[66]. This was possible due to the small width of the spectral lines. In general, the ground state of the $Er^{3+}$ ion ($^4I_{15/2}$) in a crystal field with $T_d$ symmetry will split into two doublets $\Gamma_6$ and $\Gamma_7$ and three $\Gamma_8$ quadruplets; and the first excited state ($^4I_{13/2}$) splits into $2\Gamma_6 + \Gamma_7 + 2\Gamma_8$. As a result, at low temperatures, five PL lines are expected. A lower symmetry crystal field splits the quartets into doublets. In this case, eight spectral components will appear, with each PL line corresponding to a transition between effective spin doublets.

Fig. 5 shows the Zeeman effect for the main line ($L_1^1$) of the Er-1 PL spectrum. In magnetic fields of up to 5.25 T, the splitting into seven components for $\mathbf{B}\|\langle 011\rangle$ [Fig. 5(a)] and three components for $\mathbf{B}\|\langle 100\rangle$ [Fig. 5(b)] is clearly seen. The angular dependence of line positions for the magnetic field rotated in the (011) plane is presented in the inset to Fig. 5(b). The Zeeman splitting of line $L_2^1$, $L_3^1$, $L_4^1$, and $L_1^2$ was also investigated [64]. The overall splitting of line $L_4^1$ was about an order of magnitude larger than that for $L_1^1$. Unlike in the case of $L_1^1$, transitions were observed with the difference and also with the sum of the effective $g$-factors of the excited and ground states [64]–[66]. From the analysis of the angular dependence of the magnetic field induced splitting of PL lines, the orthorhombic-I symmetry ($C_{2v}$) of the Er-1 center has been established, and individual $g$-tensors for several crystal field split levels within ground ($J = 15/2$) and excited ($J = 13/2$) state multiplets have been determined.

Although the lower-than-cubic symmetry of the Er-1 center was concluded from experiment, the distortion from cubic symmetry was small. Consequently, the observed optical transitions followed selection rules for $T_d$ rather than $C_{2v}$ symmetry. It was speculated that the observed orthorhombic-I symmetry could arise from a distortion of a tetrahedrally coordinated $Er^{3+}$ ion. If only a small distortion of cubic symmetry is present, the average $g_{av}$ factor can be related to the isotropic cubic $g_c$ factor by [67]

$$g_{av} = g_c = 1/3(g_x + g_y + g_z). \quad (1)$$

In the case of line $L_1^1$, the average $g_{av}$ value for the lowest level of the ground state is $6.1 \pm 0.5$, slightly smaller than

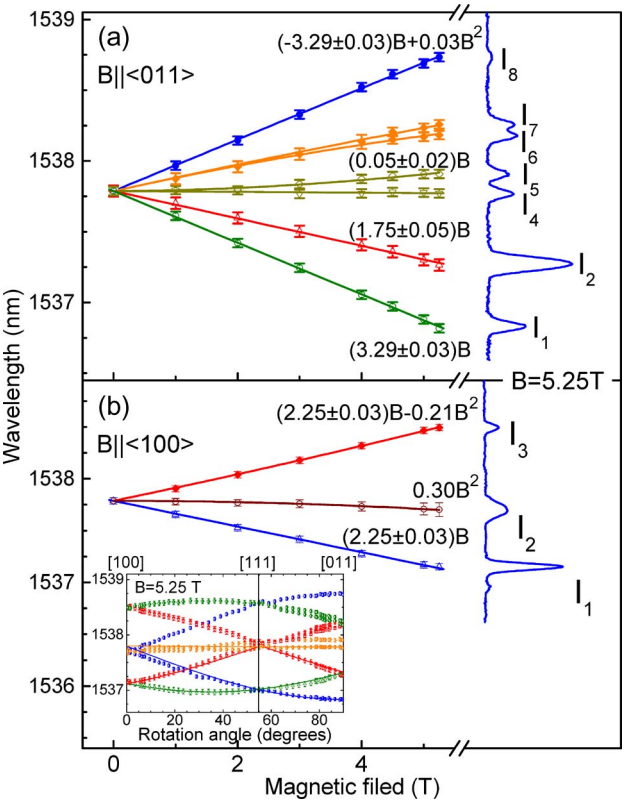


**Fig. 5.** ***Magnetic field induced splitting of the main PL line $L_1^1$ at $T = 4.2$ K for (a) $\mathbf{B}\|\langle 011\rangle$ and (b) $\mathbf{B}\|\langle 100\rangle$. The angular dependence of line positions for the magnetic field of 5.25 T rotated in the (011) plane is presented in the inset.***

the 6.8 value characteristic for pure $\Gamma_6$ and similar to values found for Er in different host materials [16], [67]–[70]. Therefore the lowest level of Er-1 ground state is likely to be of the $\Gamma_6$ character. The observed splitting is consistent with an isolated $Er^{3+}$ ion. Taking into account all the available information, the Er-1 center is identified with an $Er^{3+}$ ion occupying a slightly distorted $T_d$ interstitial site, surrounded by possibly up to eight O atoms (Fig. 6) [66].

## B. Optical Properties of Er-1 Center

*1) Decay Kinetics:* The decay characteristics of the $L_1^1$, $L_2^1$, and $L_3^1$ lines at $T = 4.2$ K under pulsed excitation at $\lambda_{exc} = 520$ nm and photon flux $\Phi = 3 \times 10^{22}$ cm$^{-2}$s$^{-1}$ are shown in Fig. 7(a). As can be seen, the decay kinetics are similar and contain a fast and a slow component. By fitting of the measured profiles, decay times of $\tau_F \approx 0.310$ ms and $\tau_S \approx 1$ ms are obtained. These values are similar to those commonly found for Si:Er structures prepared by implantation [37]. The intensity ratio of the fast and slow components is 1 : 1, the same for all the emission lines. The presence of two components in decay kinetics could indicate two different centers [71]. To examine this

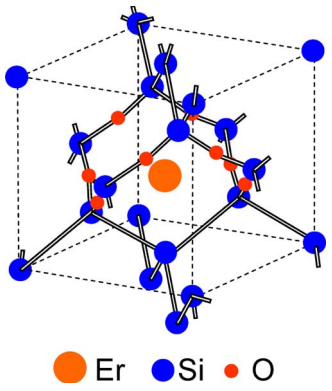


**Fig. 6.** ***The possible microscopic structure of the Er-1 center: tetrahedral interstitial $T_d$ $Er^{3+}$ ion–oxygen cluster.***

possibility, PL spectra for the fast and the slow components were separated by integrating the signal over time windows $0 < t < 100$ $\mu$s for the fast and 100 $\mu$s $< t < 4$ ms for the slow components. Both spectra were found to be identical. Taken together with the small linewidth, this result excludes the possibility of a coexistence of two different Er-related centers. The intensity ratio of the fast to the slow components was found to increase with the laser power, which suggests the participation of two different de-excitation processes. The slow component is likely to represent the radiative decay time of the Er-1, and the fast component corresponds to an Auger process with free carriers generated by the excitation pulse [42], [72].

*2) Excitation Cross-Section:* It is important to check whether the specific Er-1 center has the relatively large excitation cross-section characteristics for Er in Si. This can be evaluated from the power dependence of PL intensity.

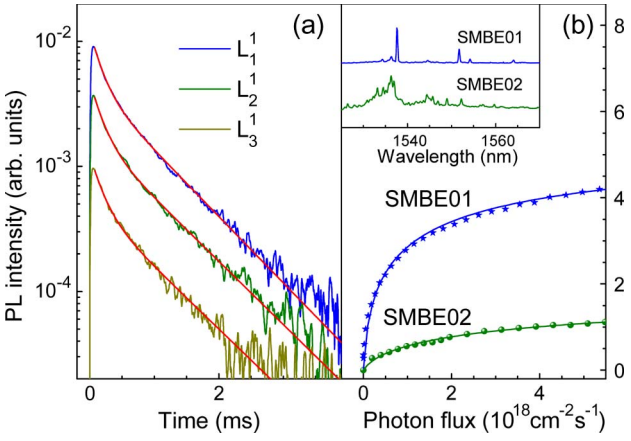


**Fig. 7.** ***(a) Decay dynamics of the Er-1 related PL under pulsed excitation ($\lambda_{exc} = 520$ nm) and (b) PL intensity dependence on excitation flux of two different multinanolayer structures at 4.2 K (details can be found in the text). The inset shows the PL spectra.***

In Fig. 7(b), the power dependence of the PL intensity for two SMBE samples is shown. One is optimized for preferential formation of the Er-1 center (SMBE01) and the other for the maximum total PL intensity (SMBE02). The total Er areal densities are $2 \times 10^{14}$ and $2 \times 10^{13}$ cm$^{-2}$ for structures SMBE01 and SMBE02, respectively. Their PL spectra, as obtained under continuous-wave excitation ($\lambda_{exc} = 514.5$ nm) at $T = 4.2$ K, are shown in the inset. The dependence of PL intensity on excitation flux is well described with the formula

$$I_{PL} = \frac{A\sigma\tau\Phi}{1 + \beta\sqrt{\sigma\tau\Phi} + \sigma\tau\Phi} \tag{2}$$

where $\sigma$ is the effective excitation cross-section of the Er-1 center, $\tau$ is the effective lifetime of $Er^{3+}$ in the excited state, and $\Phi$ is the flux of photons [41], [47], [63]. The appearance of the $\beta\sqrt{\sigma\tau\Phi}$ term, with an adjustable parameter $\beta$, is the fingerprint of an Auger effect hindering the luminescence. The solid curves represent the best fits to the experimental data using (2). For SMBE01, we get $\sigma_{cw}^{SMBE01} = (5 \pm 2) \times 10^{-15}$ cm$^2$ (identical) for all the Er-1 related lines with the Auger process related parameter $\beta = 2.0 \pm 0.1$. For sample SMBE02, the best fit is obtained for $\sigma_{cw}^{SMBE02} = (2 \pm 1) \times 10^{-15}$ cm$^2$ and $\beta = 2.0 \pm 0.1$. The values of $\sigma$ are similar to those reported for Er-implanted Si [37], [41] and indicate that the Er-1 center is activated by a similar excitation mechanism.

*3) Optical Activity:* As discussed in Section I-B1, the level of optical activity is an essential parameter of Er-doped structures determining their application potential. In order to quantify the intensity of the Er-related emission from multinanolayers and establish the optical activity level, an $SiO_2$:Er implanted sample, labeled for further reference as STD, was used. Its preparation conditions were chosen such as to achieve the full optical activation of all Er dopants and to minimize nonradiative recombination [3], [73]. The measured decay time of Er-related emission was $\tau_{STD} \approx 13$ ms, consistent with the dominance of the radiative process.

The estimation of the number of excitable centers was made by comparing the saturation level of PL intensities of STD (direct excitation at 520 $\mu$m) and SMBE samples (SMBE01 and SMBE02)—see Fig. 8. Taking into account the differences in the PL spectra, decay kinetics (nonradiative and radiative), extraction efficiencies, and excitation cross-sections, optical activities of $2 \pm 0.5\%$ for SMBE01 and $15 \pm 5\%$ for SMBE02 were determined. Therefore, the percentage of photon-emitting Er dopants obtained for the Si/Si:Er multinanolayers is comparable to that achieved in the best Si:Er materials prepared by ion implantation. In view of the relatively long radiative lifetime of Er used for concentration evaluation, the estimated percentages represent just the lower limits [63].

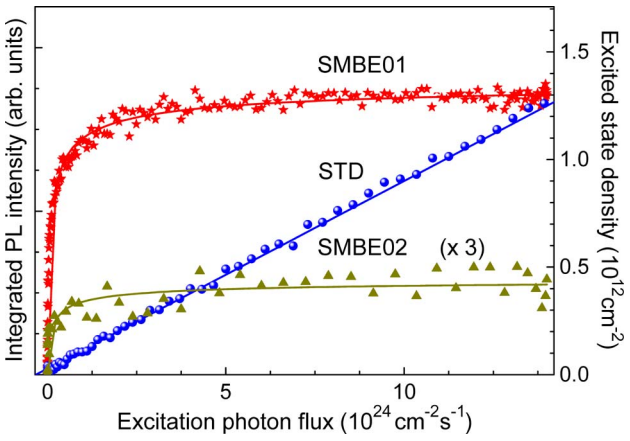


**Fig. 8.** *Intergrated PL intensity dependence of multinanolayer structures and the $SiO_2$:Er "standard" on excitation photon flux at 4.2 K.*

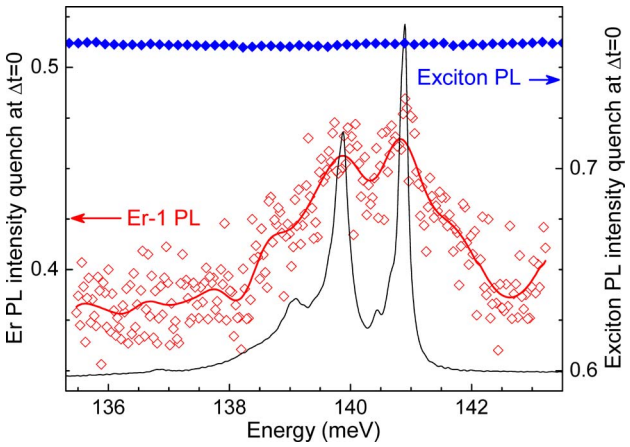


**Fig. 9.** *Results of two-color experiments at 4.2 K for Er-1 (♢) and exciton PL (♦). For comparison, the IR absorption spectrum at $T = 55$ K (black trace) of the sample is also given.*

Alternatively, the fraction of $Er^{3+}$ ions that participate in the radiative recombination can be estimated from the linear part of the excitation power dependence under pulsed excitation. Such an approach seems more appropriate, since it allows one to avoid various cooperative processes appearing in the saturation regime. The linear component for SMBE samples is taken as a derivative for photon flux $\Phi \approx 0$ of the fitting curves depicted in Fig. 8. These values are scaled with the linear dependence found for the $SiO_2$ : Er standard sample STD. When corrected for the shape of individual spectra, the lifetime, and with the average excitation cross-section, the upper limit of the total concentration of excitable $Er^{3+}$ ions is estimated as 25 ± 10% and 48 ± 20% for samples SMBE01 and SMBE02, respectively [63].

*4) Effect of 8.8 $\mu$m Oxygen Local Vibration:* The special role of O in the PL of Er, discussed earlier, can be directly demonstrated in case of the Er-1 center. To this end, a tunable mid-IR free electron laser (FEL)[2] [39], [74]–[75] was used to activate the antisymmetric vibration mode of O in Si ($\nu_3$ mode) at 8.80 $\mu$m (141 meV), and its effect was monitored on the Er-1 emission, as induced by the Nd:YAG laser used as a band-to-band pumping source. The results of this two-color experiment (depicted in Fig. 9) show the quenching ratio of Er PL as function of the photon energy of the FEL [76]. A clear resonant feature is observed for FEL wavelength around 8.80 $\mu$m (141 meV), which coincides with the oxygen-related vibrational absorption band (black trace). The reason for this effect is that the oxygen vibration induced by the FEL increases the local temperature, which results in quenching of the Er PL but negligibly increases the temperature of the whole layer, thus leaving the exciton related PL practically unaltered—see Fig. 9. In that way, the resonant quenching of the Er PL upon activation of oxygen vibrational modes evidences the spatial correlation of both dopants [76]. On the other hand, the presence of Er is also likely to influence the vibrational properties of oxygen. This could manifest itself as a shift (or, more likely, a broadening) of the 8.80 $\mu$m (141 meV) absorption band and/or a change of its vibrational time. In the relevant experiment [77], only the latter effect has been observed. Fig. 10 shows a comparison between the vibrational lifetimes of Si-O-Si modes in the investigated multinanolayer structure and in Er-free oxygen-rich Si. As can be concluded, a clear difference appears: there are two components ($\tau_{\text{fast}} = 11$ ps and $\tau_{\text{slow}} = 39$ ps) of the decay dynamics for the 8.8 $\mu$m mode in the Si/Si:Er sample versus only a single component of $\tau = 11$ ps for the Er-free material [76], [78]. The

[2]www.rijnh.nl.

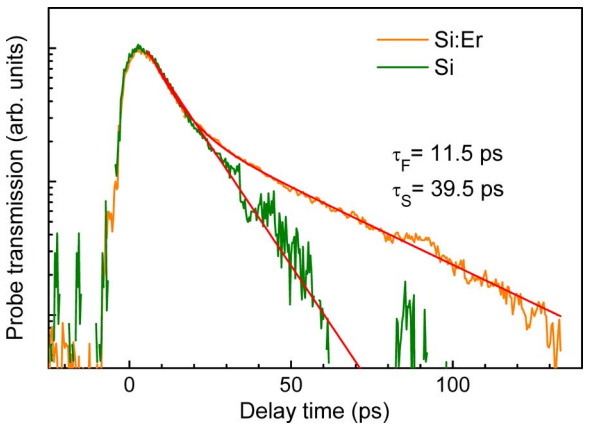


**Fig. 10.** *The change in probe transmission induced by the pump as a function of the time delay between pump and probe ($T = 10$ K) observed for the Si-O-Si local vibrational mode in the investigated multinanolayer structure (circles) and in Er-free O-rich c-Si (triangles). The pump and probe photon energy is 140.9 meV (1136.4 cm$^{-1}$).*

appearance of a slow component can be explained by the influence of the heavier mass of Er on vibrational decay dynamics of oxygen in silicon [76]. This result establishes a direct microscopic link between the intensity and thermal stability of emission of $Er^{3+}$ in Si and O doping. It also shows that the ~150 meV activation energy, commonly observed to govern the thermal stability of Er emission, corresponds to the Si-O-Si vibrational mode whose activation increases the effective temperature of the excited $Er^{3+}$ ions, promoting in this way their nonradiative recombination.

*5) Donor State and Optical Activity:* A particularly interesting feature of the Er-1 center relates to its electrical activity; for this center, the direct identification of a donor state enabling its excitation has been obtained. It was observed that the IR FEL quenches the Er-1 related PL induced by band-to-band excitation. Detailed investigations revealed [35] that the magnitude of quenching depended on the quantum energy $h\nu_{FEL}$, photon flux $\Phi_{FEL}$, and timing $\Delta t$ of the FEL pulse with respect to the band-to-band excitation. As can be seen in Fig. 11, the quenching effect appears once the photon quantum energy exceeds a certain threshold value between 210 and 250 meV and saturates at a higher photon flux with the maximum signal reduction of $Q \approx 0.35$. These characteristic features of the IR FEL induced quenching of the Er-1 PL allow identifying it with the Auger energy transfer to carriers released by the FEL pulse. Following this microscopic interpretation of the quenching mechanism, its wavelength dependence reflects the photoionization spectrum of traps releasing carriers taking part in the Auger process. From the wavelength dependence shown in Fig. 11, the ionization energy of the involved level is found as $E_D \approx 218 \pm 15$ meV [35], similar to the trap level determined for c-Si:Er by DLTS [79]. Moreover, taking the maximum quenching to be 35% of the original signal and the IR FEL pulse width of 5 $\mu$s, and using the frequently quoted value of the Auger coefficient for free electrons of $C_A \approx 10^{-13}$–$10^{-12}$ $cm^3s^{-1}$ [37], a trap concentration of $10^{17}$–$10^{18}$ $cm^{-3}$ can be concluded. This concentration is much higher than the donor or acceptor doping level of the matrix and can only be compared to the concentration of Er-related donors found in oxygen-rich Cz-Si [80]. Therefore, it appears that the FEL ionizes electrons from the donor level associated with $Er^{3+}$ ions.

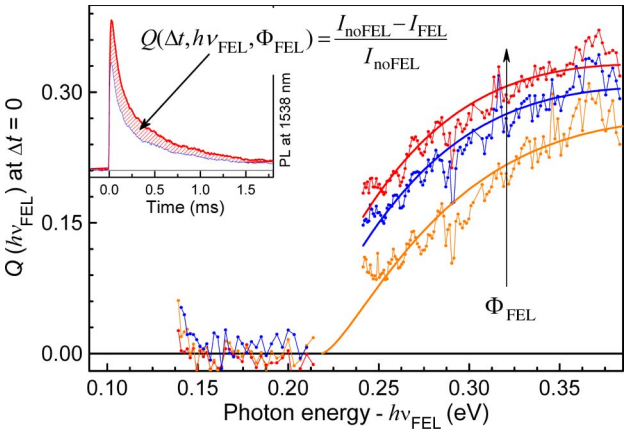


**Fig. 11.** ***FEL wavelength dependence of the induced quenching ratio of Er-related PL at 1.5 $\mu$m ($T = 4.2$ K) for several flux settings of the FEL. Solid lines correspond to simulations [33]. The inset illustrates the FEL-induced quenching effect.***

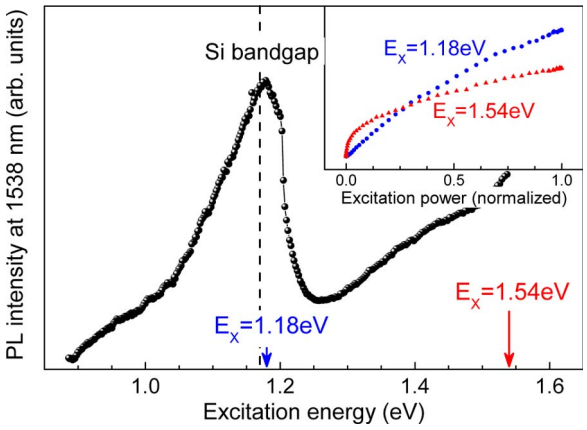


**Fig. 12.** ***PLE spectrum of the 1.5 $\mu$m Er-related emission at 4.2 K. The normalized power dependence of the PL intensity is given in the inset for two excitation wavelengths indicated by arrows.***

This conclusion was indeed confirmed by PLE spectroscopy. In Fig. 12, we present a PLE spectrum of the Er-related emission measured in the investigated structure for excitation energy close to the bandgap of c-Si. As can be seen, in addition to the usually observed contribution produced by (the onset of) the band-to-band excitation, a resonant feature, peaking at the energy around 1.18 eV, is also clearly visible. This can be identified with the resonant excitation into the Er-related bound exciton state induced by the donor revealed in the previously discussed two-color experiment. This conclusion is directly supported by the power dependence of the PL intensity, shown in the inset of Fig. 12, for the two photon energies indicated by arrows. While the data obtained for the higher energy value of 1.54 eV exhibit the saturating behavior characteristic of the band-to-band excitation mode [38], the dependence for excitation energy at 1.18 eV has a strong linear component superimposed on this saturating background. Such a linear dependence is expected for "direct" pumping.

We conclude that the results obtained in two-color and PLE spectroscopies explicitly demonstrate that the optical activity of Er in c-Si is related with a gap state. Taking advantage of the preferential formation of a single optically active Er-related center in Si/Si:Er multinanolayer structures, we determined the ionization energy of this state as $E_D \approx 218$ meV. This level provides indeed the gateway for

$Er^{3+}$ excitation as demonstrated by 1.5 $\mu$m emission upon resonant pumping into the bound exciton state of the identified donor, allowing excitation of $Er^{3+}$ while avoiding Auger quenching by free carriers.

*6) Optical Terahertz Transition Within the Ground State:* In the past, the use of optical transitions between individual levels within a single *J*-multiplet of an RE ion has been considered for generation of terahertz radiation. This approach turned out to be unsuccessful due to large width, and therefore mutual overlap, of emission lines from individual crystal-field-split levels. As mentioned, the crystal field induced splitting between sublevels of the Er-1 ground state $^4I_{15/2}$ has been precisely determined—see the inset of Fig. 4(b). On this basis, the wavelengths of the possible terahertz transitions could be predicted; in particular, one of these should take place at $\lambda \approx 43$ $\mu$m, as indicated in Fig. 4(b). This has been investigated in detail [81], and the results obtained in pump-probe experiments are shown in Fig. 13. The (normalized) traces for two wavelengths of $\lambda = 43.5$ and 42.5 $\mu$m, i.e., "on" and "off" the expected resonance, are compared. For $\lambda = 43.5$ $\mu$m, the relevant decay time constant of $\tau = 50 \pm 5$ ps is observed, superimposed on a faster decaying signal ($\tau_F \approx 10$ ps). As can be seen from the wavelength dependence of the time constant dominating the absorption (the inset of Fig. 13), the slower decay component is resonant and centered at $\lambda \approx 43.5$ $\mu$m. Consequently, we identify the slow component with an optical absorption within the ground state of Er-1 center. (The fast component, which appeared in the whole investigated wavelength range, is an experimental artifact). To the best of our knowledge, this is the first observation of an intra-*J*-multiplet optically induced transition for any RE-doped semiconductor system. While all the past investigations of Si:Er have concerned the 1.5 $\mu$m band relevant for telecommunications, this result demonstrates that the nanoengineered Si:Er could also be relevant for the terahertz range. The value of this decay time corresponds to a nonradiative multiphonon recombination process and is similar to those found for hydrogenic transitions in Si:P and Si:B systems [82].

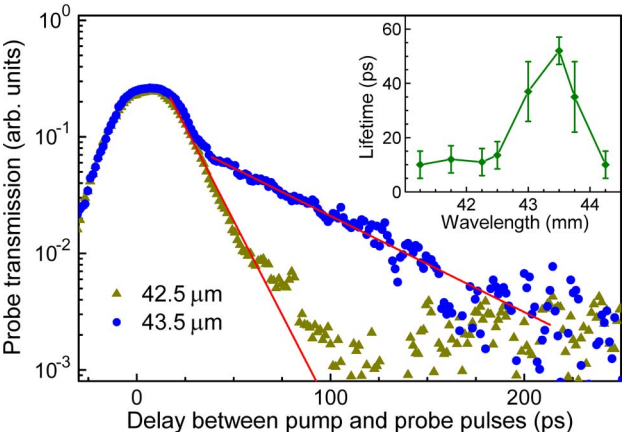


**Fig. 13.** *The change in probe transmission induced by the pump as a function of the time delay between pump and probe at the "off" and "on" resonance wavelengths—42.5 (triangles) and 43.5 $\mu$m (circles), respectively. Solid lines indicate lifetime constants of 10 and 50 ps. The inset illustrates the wavelength dependence of the time constant dominating the decay of absorption.*

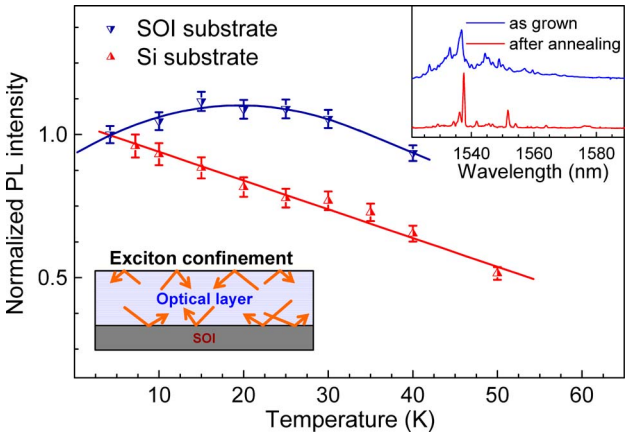


**Fig. 14.** *Temperature dependence of PL intensity from the multinanolayer structures grown on Si and SOI. The inset shows PL spectra of the sample on SOI at 4.2 K before and after annealing at 900 °C for 30 min in $N_2$.*

*7) Er-1 Center in Si/Si:Er Multinanolayers Grown on SOI Substrates:* For practical application in photonic devices, the spatial confinement of photons emitted by $Er^{3+}$ ions is necessary. For that purpose, Si/Si:Er multinanolayer structures have been grown by the similar procedure of SMBE on a semi-insulating (SOI) substrate. In this specific case, the investigated sample consisted of 20 periods of 3–6 nm Si:Er layers separated by 90 nm spacers of undoped Si [83], [84]. After an appropriate annealing process, five intense sharp PL lines typical of the Er-1 center have been observed (inset of Fig. 14).

Fig. 14 compares the temperature dependences of Er-1-related PL intensities between the multinanolayer structure grown on SOI and on Si substrates. In the structure grown on the Si substrate, the PL intensity decreases monotonously when the temperature increases, whereas, for the structure grown on SOI, the PL intensity initially increases to attain a maximum at about 15–25 K and then decreases. The initial increase of PL intensity with temperature suggests the confinement of excitons and/or free carriers within the multinanolayer structure on SOI. This is shown schematically in the inset of Fig. 14. The thermal energy detraps carriers/excitons bound to impurity centers or defects, thus generating free excitons, which enable energy transfer to unexcited Er-1 centers.

Consequently, there appears supplemental luminescence from the Er-1 centers. Such an effect is not possible in the sample grown on a Si substrate.

### C. Prospects of Optical Gain

The realization of lasing action would provide a major boost for optoelectronic applications of c-Si:Er [85]. In order to achieve gain, absorption by $Er^{3+}$ ions should be maximized and losses minimized. The latter includes absorption of the 1.5 $\mu$m radiation in the host and nonradiative recombinations of excited $Er^{3+}$ ions. For reliable gain estimation, the value of the absorption cross-section $\sigma$ at 1.5 $\mu$m for $Er^{3+}$ ions embedded in c-Si is required. This is not known and has to be derived from the linewidth $\Delta E$ and decay time $\tau$ of the 1.5 $\mu$m Er-related emission band. For the implanted Si:Er materials these are typically $\Delta E \approx 5$ meV and $\tau \approx 1$ ms. Using these values and assuming that the $\tau \approx 1$ ms time constant represents the purely radiative lifetime, the $Er^{3+}$ ion excitation cross-section can be estimated as $\sigma \approx 2.5 \times 10^{-19}$ cm$^2$. In order to calculate the gain $\alpha$, the excitation cross-section has to be multiplied by the available concentration of excited $Er^{3+}$ ions

$$\alpha(\lambda \approx 1.5\ \mu\text{m}) = \sigma(\lambda \approx 1.5\ \mu\text{m}) N(\text{Er}^*). \qquad (3)$$

Assuming a typical concentration of $Er^{3+}$ ions in the implanted layer to be $N(\text{Er}) \approx 10^{20}$ cm$^{-3}$ and taking into account that usually only ~1% of them are optically active, we obtain a gain coefficient of $\alpha \approx 0.25$ cm$^{-1}$. On the other hand, losses due to free-carrier absorption at 1.5 $\mu$m, nonradiative recombination of $Er^{3+}$ ions (Auger effect, up-conversion, etc.), are usually estimated as at least 1 cm$^{-1}$. Therefore, realization of an Si laser based on Er doping is considered unlikely.

For the Er-1 center, the ultrasmall bandwidth of its emission has dramatic consequences for the expected gain coefficient, offering a possibility to increase the excitation cross section by at least a factor $10^3$. The resulting gain coefficient should improve even more, as the percentage of optically active Er species seems to be higher for Er-1 than that in implanted samples. If we assume that the losses in the nanolayers structure are not increased, a net gain should appear.

In order to investigate that possibility, variable stripe length (VSL) and shifted excitation spot (SES) [86], [87] measurements have been conducted in an SMBE-grown sample [84]. In Fig. 15, we present a comparison between PL intensities obtained from VSL and SES experiments. As can be seen, the integrated SES PL intensity is higher than that of the VSL case, meaning that losses are overwhelming any gain that might be generated. These losses are most probably due to absorption of the Er-1 emission induced by free carriers in the excited part of the multinanolayer structure. This issue is currently under investigation [84].

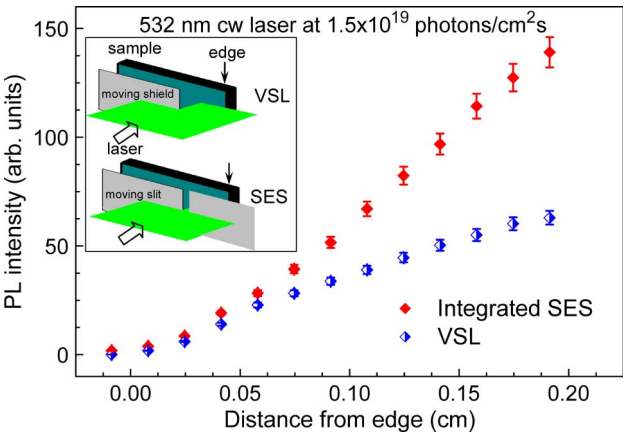


**Fig. 15.** ***Results of VSL and SES experiments for the PL intensity obtained from the multinanolayer structure at 4.2 K. The inset illustrates the principle of the SES and VSL measurements.***

## III. CONCLUSION

Demonstration of indirectly excited emission from Er-doped crystalline Si opened hopes for photonic applications of this system. In the four decades since then, an impressive amount of experimental data and theoretical results have been gathered, and many fundamental questions pertaining to this system have been satisfactorily answered. Nevertheless, important problems remain. The most prominent of these are the thermal quenching of emission and the low optical activity of the Er dopants. These preclude the application of Si:Er for the development of practical devices. The most advantageous form of Er-doped crystalline Si is currently represented by Si/Si:Er multinanolayer structures where preferential formation of a particular type of Er-related optical center has been realized. Future research will tell whether this material will allow widespread photonic applications. ■

## REFERENCES

[1] G. S. Pomrenke, P. B. Klein, and D. W. Langer, Eds., "Preface," in *Proc. MRS Symp.*, Pittsburgh, PA, 1993, vol. 301.

[2] H. Przybylińska, W. Jantsch, Y. Suprun-Belevitch, M. Stepikhova, L. Palmetshofer, G. Hendorfer, A. Kozanecki, R. J. Wilson, and B. J. Sealy, "Optically active erbium centers in silicon," *Phys. Rev. B*, vol. 54, p. 2532, 1996.

[3] A. Polman, "Erbium implanted thin film photonic materials," *J. Appl. Phys.*, vol. 82, p. 1, 1997.

[4] K. Takahei, A. Taguchi, H. Nakagome, K. Uwai, and P. S. Whitney, "Intra-4f-shell luminescence excitation and quenching mechanism of Yb in InP," *J. Appl. Phys.*, vol. 66, p. 4941, 1989.

[5] H. Ennen, J. Schneider, G. Pomrenke, and A. Axmann, "1.54-$\mu$m luminescence of erbium-implanted III-V semiconductors and silicon," *Appl. Phys. Lett.*, vol. 43, p. 943, 1983.

[6] A. J. Kenyon, "Erbium in silicon," *Semicond. Sci. Technol.*, vol. 20, p. R65, 2005.

[7] J. L. Benton, J. Michel, L. C. Kimerling, D. C. Jacobson, Y.-H. Xie, D. J. Eaglesham, E. A. Fitzgerald, and J. M. Poate,

"The electrical and defect properties of erbium-implanted silicon," *J. Appl. Phys.*, vol. 70, p. 2667, 1991.

[8] R. Serna, M. Lohmeier, P. M. Zagwijn, E. Vlieg, and A. Polman, "Segregation and trapping of erbium during silicon molecular beam epitaxy," *Appl. Phys. Lett.*, vol. 66, p. 1385, 1995.

[9] A. Karim, G. V. Hansson, and M. K. Linnarson, "Influence of Er and O concentrations on the microstructure and luminescence of Si:Er/O LEDs," *J. Phys. Conf. Ser.*, vol. 100, p. 042010, 2008.

[10] B. A. Andreev, A. Y. Andreev, H. Ellmer, H. Hutter, Z. F. Krasil'nik, V. P. Kuznetsov, S. Lanzerstorfer, L. Palmetshofer, K. Piplits, R. A. Rubtsova, N. S. Sokolov, V. B. Shmagin, M. V. Stepikhova, and E. A. Uskova, "Optical Er-doping of Si during sublimational molecular beam epitaxy," *J. Cryst. Growth*, vol. 201–202, p. 534, 1999.

[11] A. Cavallini, B. Fraboni, S. Pizzini, S. Binetti, S. Sanguinetti, L. Lazzarini, and G. Salviati, "Electrical and optical characterization of Er-doped silicon grown by liquid phase epitaxy," *J. Appl. Phys.*, vol. 85, p. 1582, 1999.

[12] Y. S. Tang, K. C. Heasman, W. P. Gillin, and B. J. Sealy, "Characteristics of rare-earth element erbium implanted in silicon," *Appl. Phys. Lett.*, vol. 55, p. 432, 1989.

[13] D. L. Adler, D. C. Jacobson, D. J. Eaglesham, M. A. Marcus, J. L. Benton, J. M. Poate, and P. H. Citrin, "Local structure of 1.54-$\mu$m-luminescence $Er^{3+}$ implanted in Si," *Appl. Phys. Lett.*, vol. 61, p. 2181, 1992.

[14] F. d'Acapito, S. Mobilio, S. Scalese, A. Terrasi, G. Franzò, and F. Priolo, "Structure of Er-O complexes in crystalline Si," *Phys. Rev. B*, vol. 69, p. 153310, 2004.

[15] M. B. Huang and X. T. Ren, "Evidence of oxygen-stabilized hexagonal interstitial erbium in silicon," *Phys. Rev. B*, vol. 68, p. 033203, 2003.

[16] J. D. Carey, R. C. Barklie, J. F. Donegan, F. Priolo, G. Franzò, and S. Coffa, "Electron paramagnetic resonance and photoluminescence study of Er-impurity complexes in Si," *Phys. Rev. B*, vol. 59, pp. 2773, 1999.

[17] U. Wahl, A. Vantomme, J. De Wachter, R. Moons, G. Langouche, J. G. Marques, and J. G., Correia and ISOLDE Collaboration, "Direct evidence for tetrahedral interstitial Er in Si," *Phys. Rev. Lett.*, vol. 79, p. 2069, 1997.

[18] M. Needels, M. Schluter, and M. Lannoo, "Erbium point defects in silicon," *Phys. Rev. B*, vol. 47, p. 15533, 1993.

[19] J. Wan, Y. Ling, Q. Sun, and X. Wang, "Role of codopant oxygen in erbium-doped silicon," *Phys. Rev. B*, vol. 58, p. 10 415, 1998.

[20] M. Hashimoto, A. Yanase, H. Harima, and H. Katayama-Yoshida, "Determination of the atomic configuration of Er–O complexes in silicon by the super-cell FLAPW method," *Phys. B*, vol. 308, p. 378, 2001.

[21] A. G. Raffa and P. Ballone, "Equilibrium structure of erbium-oxygen complexes in crystalline silicon," *Phys. Rev. B*, vol. 65, pp. 121309, 2002.

[22] D. Prezzi, T. A. G. Eberlein, R. Jones, J. S. Filhol, J. Coutinho, M. J. Shaw, and P. R. Briddon, "Electrical activity of Er and Er-O centers in silicon," *Phys. Rev. B*, vol. 71, p. 245203, 2005.

[23] C. Delerue and M. Lannoo, "Description of the trends for rare-earth impurities in semiconductors," *Phys. Rev. Lett.*, vol. 67, pp. 3006, 1991.

[24] D. J. Eaglesham, J. Michel, E. A. Fitzgerald, D. C. Jacobson, J. M. Poate, J. L. Benton, A. Polman, Y.-H. Xie, and L. C. Kimerling, "Microstructure of erbium-implanted Si," *Appl. Phys. Lett.*, vol. 58, p. 2797, 1991.

[25] S. Scalese, G. Franzò, S. Mirabella, M. Re, A. Terrasi, F. Priolo, E. Rimini, C. Spinella, and A. Carnera, "Effect of O:Er concentration ratio on the structural, electrical, and optical properties of Si:Er:O layers grown by molecular beam epitaxy," *J. Appl. Phys.*, vol. 88, p. 4091, 2000.

[26] J. L. Benton, J. Michel, L. C. Kimerling, D. C. Jacobson, Y.-H. Xie, D. J. Eaglesham, E. A. Fitzgerald, and J. M. Poate, "The electrical and defect properties of erbium-implanted silicon," *J. Appl. Phys.*, vol. 70, p. 2667, 1991.

[27] F. Priolo, G. Franzò, S. Coffa, A. Polman, S. Libertino, R. Barklie, and D. Carey, "The erbium-impurity interaction and its effects on the 1.54 $\mu$m luminescence of $Er^{3+}$ in crystalline silicon," *J. Appl. Phys.*, vol. 78, p. 3874, 1995.

[28] K. Thonke, K. Pressel, G. Bohnert, A. Stapor, J. Weber, M. Moser, A. Molassioti, A. Hangleiter, and F. Scholz, "On excitation and decay mechanisms of the $Yb^{3+}$ luminescence in InP," *Semicond. Sci. Technol.*, vol. 5, p. 1124, 1990.

[29] P. S. Whitney, K. Uwai, H. Nakagome, and K. Takahei, "Electrical properties of ytterbium-doped InP grown by metalorganic chemical vapor deposition," *Appl. Phys. Lett.*, vol. 53, p. 2074, 1988.

[30] G. Davies, T. Gregorkiewicz, M. Z. Iqbal, M. Kleverman, E. C. Lightowlers, N. Q. Vinh, and M. Zhu, "Optical properties of a silver-related defect in silicon," *Phys. Rev. B*, vol. 67, p. 235111, 2003.

[31] N. Q. Vinh, J. Phillips, G. Davies, and T. Gregorkiewicz, "Time-resolved free-electron laser spectroscopy of a copper isoelectronic center in silicon," *Phys. Rev. B*, vol. 71, p. 085206, 2005.

[32] I. N. Yassievich and L. C. Kimerling, "The mechanisms of electronic excitation of rare earth impurities in semiconductors," *Semicond. Sci. Technol.*, vol. 8, p. 718, 1993.

[33] S. Libertino, S. Coffa, G. Franzò, and F. Priolo, "The effects of oxygen and defects on the deep-level properties of Er in crystalline Si," *J. Appl. Phys.*, vol. 78, p. 3867, 1995.

[34] V. F. Masterov and L. G. Gerchikov, "The possible mechanism of excitation of the f-f emission from Er-O clusters in silicon," *Rare Earth Doped Semiconductors II*, vol. 422, S. Coffa, A. Polman, and R. N. Schwartz, Eds. Pittsburgh, PA: Materials Research Society, 1996, p. 227.

[35] I. Izeddin, M. A. J. Klik, N. Q. Vinh, M. S. Bresler, and T. Gregorkiewicz, "Donor-state-enabling Er-related luminescence in silicon: Direct identification and resonant excitation," *Phys. Rev. Lett.*, vol. 99, p. 077401, 2007.

[36] M. S. Bresler, O. B. Gusev, B. P. Zakharchenya, and I. N. Yassievich, "Exciton excitation mechanism for erbium ions in silicon," *Phys. Solid State*, vol. 38, p. 813, 1996.

[37] F. Priolo, G. Franzò, S. Coffa, and A. Carnera, "Excitation and nonradiative deexcitation processes of $Er^{3+}$ in crystalline Si," *Phys. Rev. B*, vol. 57, p. 4443, 1998.

[38] O. Gusev, M. S. Bresler, P. E. Pak, I. N. Yassievich, M. Forcales, N. Q. Vinh, and T. Gregorkiewicz, "Excitation cross section of erbium in semiconductor matrices under optical pumping," *Phys. Rev. B*, vol. 64, p. 075302, 2001.

[39] I. Tsimperidis, T. Gregorkiewicz, H. H. P. T. Bekman, and C. J. G. M. Langerak, "Direct observation of the two-stage excitation mechanism of Er in Si," *Phys. Rev. Lett.*, vol. 81, p. 4748, 1998.

[40] B. P. Pawlak, N. Q. Vinh, I. N. Yassievich, and T. Gregorkiewicz, "Influence of p-n junction formation at a Si/Si:Er interface on low-temperature excitation of $Er^{3+}$ ions in crystalline silicon," *Phys. Rev. B*, vol. 64, p. 132202, 2001.

[41] D. T. X. Thao, C. A. J. Ammerlaan, and T. Gregorkiewicz, "Photoluminescence of erbium-doped silicon: Excitation power and temperature dependence," *J. Appl. Phys.*, vol. 88, p. 1443, 2000.

[42] N. Q. Vinh, "Optical properties of isoelectronic centers in crystalline silicon," Ph.D. dissertation, University of Amsterdam, Amsterdam, The Netherlands, 2004.

[43] T. Gregorkiewicz, D. T. X. Thao, and J. M. Langer, "Direct spectral probing of energy storage in Si:Er by a free-electron laser," *Appl. Phys. Lett.*, vol. 75, p. 4121, 1999.

[44] M. Forcales, T. Gregorkiewicz, M. S. Bresler, O. B. Gusev, I. V. Bradley, and J.-P. Wells, "Microscopic model for nonexcitonic mechanism of 1.5-$\mu$m photoluminescence of the $Er^{3+}$ ion in crystalline Si," *Phys. Rev. B*, vol. 67, p. 085303, 2003.

[45] T. Gregorkiewicz, I. Tsimperidis, C. A. J. Ammerlaan, F. P. Widdershoven, and N. A. Sobolev, "Excitation and de-excitation of $Yb^{3+}$ in InP and $Er^{3+}$ in Si: Photoluminescence and impact ionization studies," *Proc. Mater. Res. Soc. Symp.*, vol. 422, p. 207, 1996.

[46] J. M. Langer, "Localized center luminescence quenching by the Auger effect," *J. Lumin.*, vol. 40–41, p. 589, 1988.

[47] J. Palm, F. Gan, B. Zheng, J. Michel, and L. C. Kimerling, "Electroluminescence of erbium-doped silicon," *Phys. Rev. B*, vol. 54, p. 17603, 1996.

[48] A. S. Moskalenko, I. N. Yassievich, M. Forcales, M. A. J. Klik, and T. Gregorkiewicz, "Terahertz-assisted excitation of the 1.5-$\mu$m photoluminescence of Er in crystalline Si," *Phys. Rev. B*, vol. 70, p. 155201, 2004.

[49] M. S. Bresler, O. B. Gusev, O. E. Pak, and I. N. Yassievich, "Efficient Auger-excitation of erbium electroluminescence in reversely-biased silicon structures," *Appl. Phys. Lett.*, vol. 75, p. 2617, 1999.

[50] I. Izeddin, A. S. Moskalenko, I. N. Yassievich, M. Fujii, and T. Gregorkiewicz, "Nanosecond dynamics of the near-infrared photoluminescence of Er-doped $SiO_2$ sensitized with Si nanocrystals," *Phys. Rev. Lett.*, vol. 97, p. 207401, 2006.

[51] I. Izeddin, D. Timmerman, T. Gregorkiewicz, A. A. Prokofiev, A. S. Moskalenko, I. N. Yassievich, and M. Fujii, "Energy transfer in Er-doped $SiO_2$ sensitized with Si nanocrystals," *Phys. Rev. B*, vol. 78, p. 035327, 2008.

[52] D. Timmerman, I. Izeddin, P. Stallinga, I. N. Yassievich, and T. Gregorkiewicz, "Space-separated quantum cutting with silicon nanocrystals for photovoltaic applications," *Nature Phot.*, vol. 2, p. 105, 2008.

[53] H. Vrielinck, I. Izeddin, V. Y. Ivanov, T. Gregorkiewicz, F. Callens, D. S. Lee, A. J. Steckl, and N. M. Khaidukov, "Erbium doped silicon single- and multilayer structures for LED and laser applications," in *Proc. MRS. Symp.*, 2005, vol. 866, p. 13.

[54] E. Snoeks, A. Lagendijk, and A. Polman, "Measuring and modifying the spontaneous emission rate of erbium near an interface," *Phys. Rev. Lett.*, vol. 74, p. 2459, 1995.

[55] A. Karim, W. -X. Ni, A. Elfvink, P. O. Å. Persson, and G. V. Hansson, "Characterization of Er/O-doped Si-LEDs with low thermal quenching," in *Proc. Mater. Res. Soc. Symp.*, 2005, vol. 866, V4.2.1/FF4.2.1.

[56] A. Taguchi, K. Takahei, and J. Nakata, "Electronic properties and their relations to optical properties in rare earth doped III-V semiconductors," *Rare Earth Doped Semiconductors*, vol. 301, G. S. Pomrenke, P. B. Klein, and D. W. Langer, Eds. Pittsburgh, PA: Materials Research Society, 1993, vol. 301, p. 139.

[57] M. A. J. Klik, T. Gregorkiewicz, I. V. Bradley, and J.-P. Wells, "Optically induced deexcitation of rare-earth ions in a semiconductor matrix," *Phys. Rev. Lett.*, vol. 89, p. 227401, 2002.

[58] A. A. Prokofiev, I. N. Yassievich, H. Vrielinck, and T. Gregorkiewicz, "Theoretical modeling of thermally activated luminescence quenching processes in Si:Er," *Phys. Rev. B*, vol. 72, p. 045214, 2005.

[59] M. Forcales, T. Gregorkiewicz, and M. S. Bresler, "Auger deexcitation of $Er^{3+}$ ions in crystalline Si optically induced by midinfrared illumination," *Phys. Rev. B*, vol. 68, p. 035213, 2003.

[60] V. P. Kuznetsov, A. Y. Andreev, O. A. Kuznetsov, L. E. Nikolaeva, T. M. Sotova, and N. V. Gudkova, "Heavily doped Si layers grown by molecular beam epitaxy in vacuum," *Phys. Status Solidi A*, vol. 127, p. 371, 1991.

[61] M. V. Stepikhova, B. A. Andreev, V. B. Shmagin, Z. F. Krasil'nik, V. P. Kuznetsov, V. G. Shengurov, S. P. Svetlov, W. Jantsch, L. Palmetshofer, and H. Ellmer, "Properties of optically active Si:Er and $Si_{1-x}Ge_x$ layers grown by the sublimation MBE method," *Thin Solid Films*, vol. 369, p. 426, 2000.

[62] W. Jantsch, S. Lanzerstorfer, L. Palmetshofer, M. Stepikhova, and H. Preier, "Different Er centres in Si and their use for electroluminescent devices," *J. Lumin.*, vol. 80, p. 9, 1999.

[63] N. Q. Vinh, S. Minissale, H. Vrielinck, and T. Gregorkiewicz, "Concentration of $Er^{3+}$ ions contributing to 1.5-$\mu$m emission in Si/Si:Er nanolayers," *Phys. Rev. B*, vol. 76, p. 085339, 2007.

[64] N. Q. Vinh, H. Przybylińska, Z. F. Krasil'nik, and T. Gregorkiewicz, "Optical properties of a single type of optically active center in Si/Si:Er nanostructures," *Phys. Rev. B*, vol. 70, p. 115332, 2004.

[65] N. Q. Vinh, H. Przybylińska, Z. F. Krasil'nik, B. A. Andreev, and T. Gregorkiewicz, "Observation of Zeeman effect in photoluminescence of $Er^{3+}$ ion imbedded in crystalline silicon," *Phys. B*, vol. 308–310, p. 340, 2001.

[66] N. Q. Vinh, H. Przybylińska, Z. F. Krasil'nik, and T. Gregorkiewicz, "Microscopic structure of Er-related optically active centers in crystalline silicon," *Phys. Rev. Lett.*, vol. 90, p. 066401, 2003.

[67] P. K. Watts and W. C. Holton, "Paramagnetic-resonance studies of rare-earth impurities in II-VI compounds," *Phys. Rev.*, vol. 173, p. 417, 1968.

[68] J. D. Kingsley and M. Aven, "Paramagnetic resonance and fluorescence of $Er^{3+}$ at cubic sites in ZnSe," *Phys. Rev.*, vol. 155, p. 235, 1967.

[69] U. Ranon and W. Low, "Electron spin resonance of $Er^{3+}$ in $CaF_2$," *Phys. Rev.*, vol. 132, p. 1609, 1963.

[70] M. J. Weber and R. W. Bierig, "Paramagnetic resonance and relaxation of trivalent rare-earth ions in calcium fluoride," *Phys. Rev.*, vol. 134, p. A1504, 1964.

[71] S. Coffa, G. Franzò, F. Priolo, A. Polman, and R. Serna, "Temperature dependence and quenching processes of the intra-4*f* luminescence of Er in crystalline Si," *Phys. Rev. B*, vol. 49, p. 16313, 1994.

[72] N. Q. Vinh, S. Minissale, B. A. Andreev, and T. Gregorkiewicz, "Auger process of luminescence quenching in Si/Si:Er multinanolayers," *J. Phys.*, vol. 17, p. S2191, 2005.

[73] A. Polman, D. C. Jacobson, D. J. Engelsham, R. C. Kistler, and J. M. Poate, "Optical doping of waveguide materials by MeV Er implantation," *J. Appl. Phys.*, vol. 70, p. 3778, 1991.

[74] M. Forcales, M. A. J. Klik, N. Q. Vinh, J. Phillips, J.-P. R. Wells, and T. Gregorkiewicz, "Two-color mid-infrared spectroscopy of optically doped semiconductors," *J. Lumin.*, vol. 102–103, p. 85, 2003.

[75] M. Forcales, T. Gregorkiewicz, I. V. Bradley, and J.-P. R. Wells, "Afterglow effect in photoluminescence of Si:Er," *Phys. Rev. B*, vol. 65, p. 195208, 2002.

[76] S. Minissale, N. Q. Vinh, W. de Boer, M. S. Bresler, and T. Gregorkiewicz, "Microscopic evidence for role of oxygen in luminescence of $Er^{3+}$ ions in Si: Two-color and pump-probe spectroscopy," *Phys. Rev. B.*, vol. 78, p. 035313, 2008.

[77] M. Califano, N. Q. Vinh, P. J. Phillips, Z. Ikonić, R. W. Kelsall, P. Harrison, C. R. Pidgeon, B. N. Murdin, D. J. Paul, P. Townsend, J. Zhang, I. M. Ross, and A. G. Cullis, "Interwell relaxation times in *p*-Si/SiGe asymmetric quantum well structures: Role of interface roughness," *Phys. Rev. B*, vol. 75, p. 045338, 2007.

[78] K. K. Kohli, G. Davies, N. Q. Vinh, D. West, S. K. Estreicher, T. Gregorkiewicz, I. Izeddin, and K. M. Itoh, "Isotope dependence of the lifetime of the 1136-$cm^{-1}$ vibration of oxygen in silicon," *Phys. Rev. Lett.*, vol. 96, p. 225503, 2006.

[79] F. P. Widdershoven and J. P. M. Naus, "Donor formation in silicon owing to ion implantation of the rare earth metal erbium," *Mater. Sci. Eng. B*, vol. 4, p. 71, 1989.

[80] F. Priolo, S. Coffa, G. Franzò, C. Spinella, A. Carnera, and V. Bellani, "Electrical and optical characterization of Er-implanted Si: The role of impurities and defects," *J. Appl. Phys.*, vol. 74, p. 4936, 1993.

[81] S. Minissale, N. Q. Vinh, A. F. G. van der Meer, M. S. Bresler, and T. Gregorkiewicz, "Terahertz electromagnetic transitions observed within the $^4I_{15/2}$ ground multiplet of $Er^{3+}$ ions in Si," *Phys. Rev. B*, p. 115324, vol. 79, 2009.

[82] N. Q. Vinh, P. T. Greenland, K. Litvinenko, B. Redlich, A. F. G. van der Meer, S. A. Lynch, M. Warner, A. M. Stoneham, G. Aeppli, D. J. Paul, C. R. Pidgeon, and B. N. Murdin, "Silicon as a model ion trap: Time domain measurements of donor Rydberg states," *P. Nat. Acad. Sci. USA*, vol. 105, p. 10 649, 2008.

[83] Z. F. Krasil'nik, B. A. Andreev, D. I. Kryzhkov, L. V. Krasilnikova, V. P. Kuznetsov, D. Y. Remizov, V. B. Shmagin, M. V. Stepikhova, A. N. Yablonskiy, T. Gregorkiewicz, N. Q. Vinh, W. Jantsch, H. Przybylińska, V. Y. Timoshenko, and D. M. Zhigunov, "Erbium doped silicon single- and multilayer structures for light-emitting device and laser applications," *J. Mater. Res.*, vol. 21, p. 574, 2006.

[84] N. N. Ha, J. Valenta, and T. Gregorkiewicz, in preparation.

[85] T. Gregorkiewicz and J. M. Langer, "Lasing in rare-earth-doped semiconductors: Hopes and facts," *MRS Bull.*, vol. 24, pp. 27–31, 1999.

[86] K. L. Shaklee and R. F. Leheny, "Direct determination of optical gain in semiconductor crystals," *Appl. Phys. Lett.*, vol. 18, p. 475, 1971.

[87] J. Valenta, K. Luterova, R. Tomasiuas, K. Dohnalova, B. Honerlage, and I. Pelant, *Towards the First Silicon Laser*, L. Pavesi, S. Gaponenko, and L. DalNegro, Eds. Norwell, MA: Kluwer, 2003.

## ABOUT THE AUTHORS

**Nguyen Quang Vinh** received the B.Sc. degree in engineering physics from the Hanoi University of Technology, Hanoi, Vietnam, in 1996 and the M.Sc. degree from the Institute of Physics, Hanoi, in 1999. He received the Ph.D. degree in physics from the University of Amsterdam, Amsterdam, The Netherlands, in 2004

He is presently at Institute for Terahertz Science and Technology, Department of Physics, University of California, Santa Barbara. Before, he was a Senior UK Facility Scientist at the Free Electron Laser for Infrared Experiment (FELIX), FOM Institute for Plasma Physics Rijnhuizen, The Netherlands. He performed his doctoral research on photonic properties of Er-doped crystalline silicon. He is currently investigating dynamic processes and energy transfers in low-dimensional semiconductor structures and condensed phase systems using ultrafast lasers from the violet to far-infrared range for use in photodetectors, emitters, and quantum information processes.

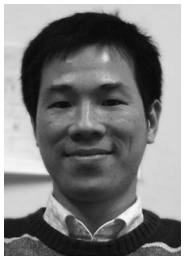

**Ngo Ngoc Ha** received the B.Sc. degree in physics from Hanoi University of Natural Sciences, in 2001 and the M.Sc. degree in materials science from the International Training Institute for Materials Science, Hanoi University of Technology, Hanoi, in 2003, in Vietnam. He is currently pursuing the Ph.D. program at the Van der Waals-Zeeman Institute, University of Amsterdam, the Netherlands.

His research concerns optical properties of Si/Si:Er nanomultilayers grown by SMBE method for Si-based photonic application, and in particular optical gain at low temperature.

**Tom Gregorkiewicz** received the M.S. degree in physics from the Warsaw University, Poland, and the Ph.D. degree from the Institute of Physics, Polish Academy of Sciences.

In 1989, he joined the Faculty Staff of the Science Department, University of Amsterdam, The Netherlands, where he currently holds the Optoelectronic Materials Chair. His research interests include the optical properties of semiconductors and, prominently, fundamental aspects of silicon photonics. His group at the Van der Waals-Zeeman Institute, University of Amsterdam, specializes in multicolor optical and resonance spectroscopy of electronic and optoelectronic nanostructured materials. Experimental techniques include, among others, two-color spectroscopy using a free-electron laser as a time-resolved source of intense terahertz-range radiation. He is an author of more than 200 refereed publications and more than 45 invited presentations at international conferences and workshops.